http://dx.doi.org/10.5012/bkcs.2014.35.12.3583

Fabrication of Mesoporous Hollow TiO_2 Microcapsules for Application as a DNA Separator

Sang Gweon Jeon, Jin Young Yang, Keun Woo Park, and Geon-Joong Kim*

*Department of Chemical Engineering, Inha University, Incheon 402-751, Korea. *E-mail: kimgj@inha.ac.kr*
Received August 7, 2014, Accepted August 25, 2014

This study evaluated a simple and useful route to the synthesis of mesoporous TiO_2 microcapsules with a hollow macro-core structure. A hydrophilic precursor sol containing the surfactants in the hydrophobic solvents was deposited on PMMA polymer surfaces modified by non-thermal plasma to produce mesoporous shells after calcination. The surface of the PMMA polymer spheres was coated with NH_4F and CTAB to control the interfacial properties and promote the subsequent deposition of inorganic sols. These hollow type mesoporous TiO_2 microcapsules could be applied as an efficient substrate for the immobilization of DNA oligonucleotides.

Key Words : TiO_2 microcapsule, DNA oligonucleotides, Hollow sphere, Mesoporous shell

Introduction

The development of effective probes with practical advantages in terms of deoxyribonucleic acid (DNA) separation with easy handling and recycling ability has attracted considerable interest.[1-3] High adsorption property of the DNA oligonucleotides to a solid substrate is needed for DNA sequencing analysis as the first step. Many techniques are currently being used for the direct confirmation of hybridization assays for DNA sequencing with the aim of upgrading the detection system.[4] On the other hand, the current methods for DNA separation have some drawbacks in the manufacture of pharmaceutical grade compounds, including the use of toxic chemicals, such as phenol, cesium chloride and ethidium bromide. In addition, further enhancement to increase the amount of DNA adsorbed is needed because the low capacity for DNA adsorption is still a common limitation. Recently Kang *et al.* reported that chemically functionalized silica-coated magnetic particles were quite efficient for the direct separation of DNA, and the adsorption efficiency of aminofunctionalized nanoparticles was 4-5 times higher than that of silica-coated ones.[5] Meier and Gratzel used nanocrystalline semiconductor oxides (nanocrystalline TiO_2 films) as substrates for immobilizing DNA oligonucleotides.[6] The oxide material of choice was anatase TiO_2, to which the nucleotide binds firmly *via* complexation of the phosphate group to the titanium ions on the matrix surfaces. Electron transfer from the conduction bands of the semiconductor oxides to adsorbed mononucleotides has been reported.[7] In the application of nanocrystalline TiO_2 films, it was claimed that the mesoporous morphology of the anatase layers offered a huge internal contact areas for the immobilization of DNA probes.

Hollow microcapsules have a number of interesting advantages for many applications, such as in adsorption, catalysis, chromatography, the protection of biologically active agents and the controlled drug delivery system because of their high surface, large hollow structure and compatibility with other materials.[8-10] The development of macroporous materials with pore sizes beyond 30 nm has been reported using a variety of templates, such as polystyrene latex spheres, oil droplets in an oil-in-water emulsion, vesicles and foams.[11-17] Some studies have reported the synthesis of spherical hollow particles with a narrow size distribution. Numerous techniques for the fabrication of inorganic hollow particles are available based on physical and chemical methods.[18-20] In a typical procedure, inorganic hollow microspheres can be synthesized by a sacrificial core method, for which nanosized inorganic particles are coated on the surfaces of polymer spheres through the controlled precipitation of inorganic precursor molecules. The template polymer microspheres are then removed by calcination in air to generate the inorganic hollow spheres.[21] Recently, mesoporous Al_2O_3 and TiO_2 microspheres with a hollow core structure and SiO_2 with a uniform morphology were synthesized using ionic liquids to modify the surfaces of the polymer template.[22,23] As a continuation of this work, attention has been paid to identifying a new route to prepare the hollow mesoporous inorganic particles under milder conditions through a simple process. This paper presents an efficient methodology for the preparation of mesoporous pure TiO_2 microcapsules with a hollow macro-core structure. To fabricate the mesoporous microcapsules, a hydrophilic inorganic precursor sol containing surfactants in hydrophobic solvents was deposited onto polymethylmetacrylate (PMMA) polymer surfaces that had been modified by a plasma treatment and NH_4F coating. The main objective of surface modification by non-thermal plasma is to oxidize the surfaces of PMMA to promote the adsorption of hydrophilic compounds, as well as for the subsequent deposition of inorganic sols. Because the inorganic precursor sol to form a MCM-41 type material was solidified rapidly in the presence of ammonia, NH_4F was coated on PMMA treated previously by non–thermal plasma. The continuous gellation of the hydrophilic sol in the hydrophobic solvents has resulted in the successful formation of corresponding mesoporous microcapsules.

This paper also reports the use of TiO_2 microcapsules with a hollow macroporous core and mesoporous shell structure as substrates for the immobilization and separation of DNA oligonucleotides. The mesoporous morphology of anatase in the hollow layers offered enhanced surfaces to greatly increase the amount of probes immobilized on the substrates. The effects of the size of the TiO_2 particles, TiO_2 contents and the porosity in the microcapsules on the adsorption rates and capacities were investigated in detail. In addition, the desorption of DNA from the TiO_2 surfaces was also tested as a function of the NaCl concentration in solution for the repeated use of TiO_2 substrates.

Experimental

Monodisperse PMMA spheres with a mean diameter of 25 μm (TAFTIC$_{TM}$ FH-S series; for use of light diffuser) were purchased from Toyobo Co. PMMA microspheres, 1.5 and 2.5 μm in size, were synthesized using a well-known polymerization method.[24] In typical, emulsion polymerization was carried out in a glass flask equipped with a three-way stopcock under nitrogen. Polyvinyl pyrrolidone (PVP, Mw = 10,000, 3.5 g) was dissolved in a methanol/water (vol/vol = 2.5, 100 mL) mixture with stirring in a nitrogen atmosphere. Subsequently, methyl methacrylate monomer (10.0 g) and initiator 2,2-azobisisobutyronitrile (AIBN, 0.1 g) were added slowly to the PVP containing solution. The reaction was conducted at 50 °C for 4 h, and the temperature was then increased slowly to 70 °C for another 20 h reaction. The emulsion sample was collected by centrifuging and repeated washed with methanol and water several times.

The synthesis of bimodal hollow TiO_2 microcapsules with mesoporous shells was performed by coating the TiO_2 sol on the PMMA core spheres, as shown in Scheme 1. Typically, in the preparation of Ti-MCM-41 precursor sol, 6.8 g of titanium(IV) chloride ($TiCl_4$; 99.9%, Aldrich) was placed into 10 g of absolute methanol (MeOH) and heated under reflux for 30 min. Acetic acid (CH_3COOH, 1 g) was then added to the mixture and heated under reflux for an additional 1 h. For the incorporation of silica, TEOS was added to the sol mixture. The Si/Ti mole ratios were fixed to 0, 0.25 or 1.0. After adding the deionized water (3 g), the mixture was heated under reflux for 2 h. The typical mole ratio of $TiCl_4$:MeOH:H_2O:CH_3COOH was 1:8.717:4.650:0.465 in the mixed solution (solution A). Separately, 8.75 g of n-hexadecyl trimethyl ammonium bromide (C_{16}TMABr; Aldrich) was dissolved in 26 g of methanol (solution B). A mixture of solutions A and B was then heated under reflux for 4 h, and the solvent was then evaporated to reduce the total solution volume by 50%. The PMMA surfaces were modified by a non-thermal plasma treatment to make the surfaces hydrophilic. Figure 1 presents the apparatus of the non-thermal plasma adopted in this work. The surfaces of plasma-treated PMMA were then coated simultaneously with 10 wt % of NH_4F and 20 wt % CTAB (basis; weight of PMMA). The corresponding amount of NH_4F and CTAB was dissolved in methanol/water (vol/vol = 1). After adding the PMMA particles (5 g) to the solution and stirring for 30 min, the solvent was removed completely under vacuum. The PMMA spheres (10 g) coated with NH_4F and CTAB were mixed in a paraffin solution (50 mL). A good dispersion of modified PMMA particles was achieved. Because NH_4F is soluble only in water, the coating layers of NH_4F were maintained on PMMA surfaces in an organic solution.

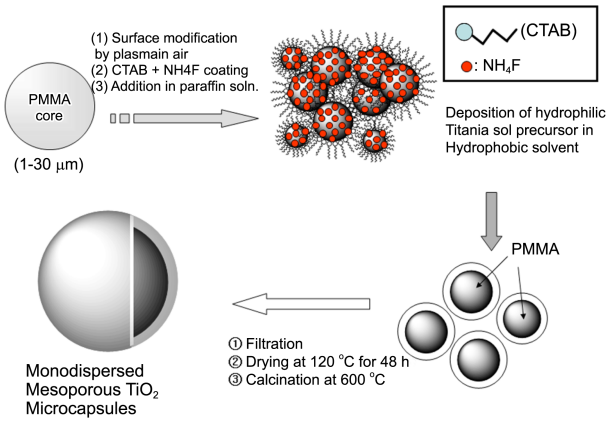

Scheme 1. Typical procedure for fabrication of bimodal hollow TiO_2 microcapsules with mesoporous shells by coating the TiO_2 sol on the PMMA core spheres.

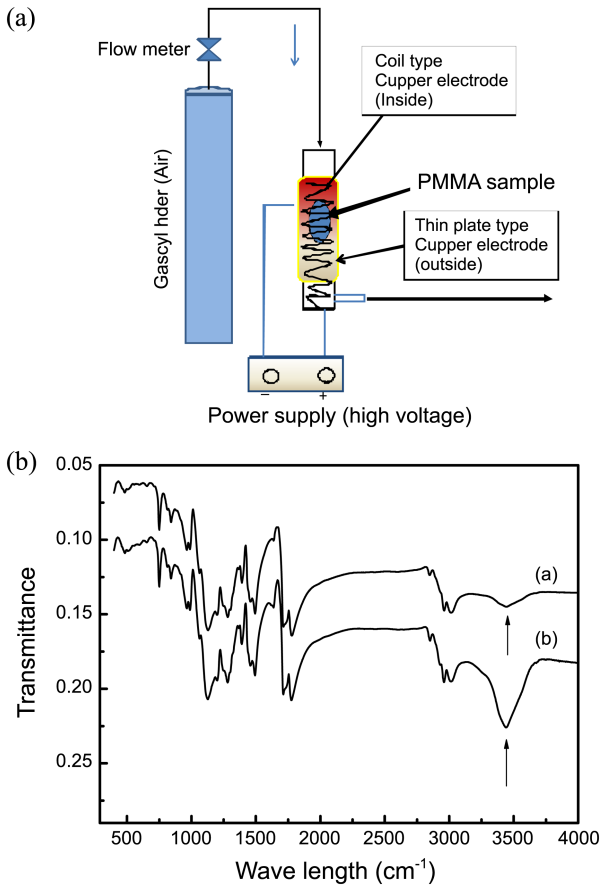

Figure 1. Non-thermal plasma apparatus adopted for the modification of PMMA surfaces to make the surfaces hydrophilic (a). FT-IR spectra of PMMA samples before and after non-thermal plasma treatment (b).

Under the full dispersion of particles in solution, the concentrated TiO_2 sol-solution (6 g) was added drop wise. The entire mixture was then stirred at room temperature for 6 h, and heated to 100 °C for 3 h. As soon as the TiO_2 and SiO_2 sol contacted the NH_4F layer, the sols solidified suddenly as a gel on the PMMA surfaces. As a final step, ammonia water (2 mL) diluted in methanol (20 mL) was added to the suspension solution to solidify the mesoporous sol into a gel, and the reaction mixture was then kept for 3 h with constant stirring. The nanoparticles formed as separated ones were removed easily during filtration and water washing. The collected composite particles were filtered, washed with various solvents and dried at 120 °C for 48 h. The precursor PMMA polymer spheres were removed by direct calcination at 600 °C for 4 h in air. The heating rate room temperature to 600 °C was 1 °C/min. For comparison, the mixture of silica and TiO_2 sol containing CTAB was coated on the modified PMMA surfaces to incorporate silica in the mesoporous hollow matrix. The hollow type nonporous TiO_2 spheres were also prepared by coating the TiO_2 sol on the modified PMMA polymer spheres. In that TiO_2 sol, no surfactant, such as CTAB, was added. The calcined hollow type solid particles were used to examine Cy5-labeled DNA adsorption.

The as-synthesized composites and calcined microcapsules were characterized by X-ray diffraction (Phillips PW 3123), field emission transmission electron microscopy (FE-TEM, S-4200) and scanning electron microscopy (FE-SEM, JEM-2100F). The nitrogen adsorption and desorption experiments were performed at −196 °C using surface area and porosity analysis equipment (Micromeritics, ASAP 2010). A zeta-potentiometer (ELS-Z model) was used to investigate the surfaces characteristics of the fresh PMMA, plasma-treated PMMA and hollow TiO_2 particles. The Cy5-labeled DNA molecules were purchased from BioNeer Corp. (Mw = 4398.3 g/mol, purified by HPLC) and used as received. Scheme 2 shows the structure of the DNA oligomer molecules. The cyanine (Cy5) group was introduced to DNA to visualize the adsorbed molecules in the microscopic images through laser excitation. They were adsorbed on the calcined mesoporous hollow TiO_2 microcapsules at 20 °C. The solution was centrifuged for 10 min at 12000 rpm, and the supernatant was collected to determine the amount of DNA adsorbed on the TiO_2 particles. The DNA concentration in solution can be calculated readily from the absorbance at 250-300 nm by UV spectroscopy. The Cy5-labeled DNA bound to the surfaces of the TiO_2 microcapsules were excited at 650 nm and their emission spectra were captured by confocal laser scanning microscopy (CLSM, LSM-510 META model). The particle samples were rinsed with 1.0 mL of distilled water and vacuum dried at 50 °C prior to CLSM analysis. In addition, the adsorption of DNA from the TiO_2 surfaces was conducted as a function of the NaCl concentration. The concentrations of NaCl salt ranged from 0.1 to 0.8 M.

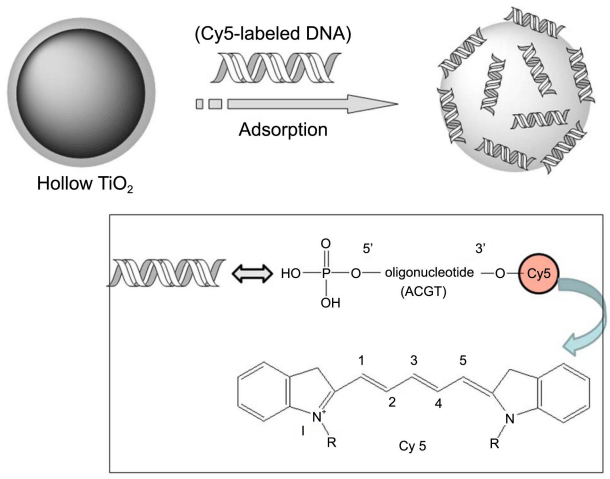

Scheme 2. The structure of the DNA oligomer molecule having a cyanine (Cy5) group to visualize the molecules by the laser excitation.

Results and Discussion

The pre-hydrolyzed TiO_2 sol-solution was coated progressively and solidified on the surfaces of the PMMA core particles to form a thick film of mesoporous TiO_2-shells, as summarized in Scheme 1. The prior modification of PMMA surfaces by coating NH_4F was critical for the successful deposition of the hydrophilic precursor (inorganic sol) on the polymer surfaces. The surfaces of the fresh PMMA were oxidized by a non-thermal plasma treatment in air to make the surfaces hydrophilic, using the apparatus shown in Figure 1. The highly hydrophilic nature of modified PMMA can be visualized as the absorption peak of OH groups on the FTIR spectra. The zeta-potential value for the fresh PMMA particles was −15.83 mV, but it was changed to −9.63 mV after the plasma-treatment. This confirms that the PMMA surfaces were oxidized in the non-thermal plasma stream. Furthermore, the dried TiO_2 microcapsules showed a very low zeta-potential (−4.22 mV) after coating on PMMA, indicating full coverage of inorganic layers on the polymer surfaces. Once the TiO_2 solid layer began to form on the PMMA surfaces through contact with NH_4F, the continuous deposition of precursor sol occurred progressively on the wall layer in the hydrophobic solvent, such as paraffin. The size of the vacant core in the hollow silica could be controlled simply by using PMMA template spheres with a different mean size. The thickness of the mesoporous wall could be controlled with increasing amount of Ti-MCM-41 precursor sol coated.

Figure 2 shows SEM images of the mesoporous TiO_2 microcapsules fabricated using PMMA spheres with diameters of 1.5 μm and 25 μm as a template. Calcination of the PMMA template at 600 °C in air generated the anatase-type TiO_2 microcapsules with a hollow core with mesoporous shell. For the synthesis of this hollow shell-type mesoporous TiO_2 material, the mesoporous shell was constructed from pure Ti-MCM-41 sol in the absence of silica sources. The surface roughness of the TiO_2 sol coated spheres indicated the formation of inorganic shells surrounding the core polymer particles. On the other hand, the outer surfaces of the resulting TiO_2 microcapsules (Fig. 2(b, c) and 2(e, f))

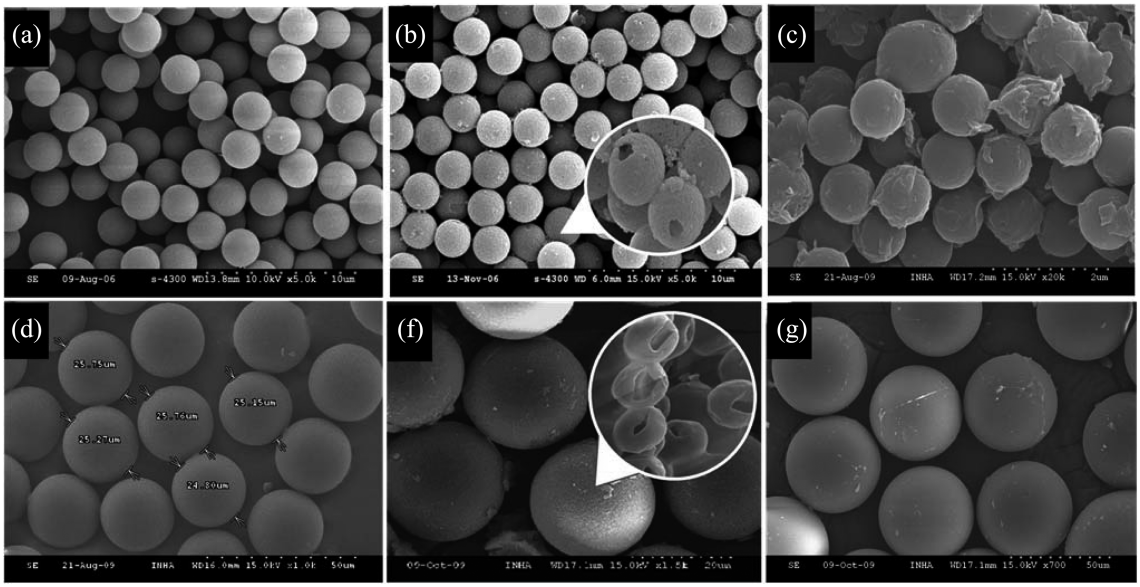

Figure 2. SEM images of the mesoporous TiO_2 microcapsules fabricated using PMMA spheres with diameters of 1.5 μm (a, b, c) and 25 μm (d, e, f) as a template.

were quite rough, showing that the thin core shells of those beads are fabricated by the primary nanoparticles, followed by progressive coagulation and condensation to generate thick walls. The photomicrographs included together in Figure 2(b) and 2(e) are showing a hollow structure with a vacant core in the partially broken sample. SEM revealed TiO_2 capsules with spherical shell structures with a wall thickness of approximately 0.1 μm and 1.5 μm when the diameters were 1.5 μm and 25 μm, respectively, after burning the core PMMA polymers by calcination in air.

The presence of the mesopores in the shell of the hollow TiO_2 was supported by XRD, TEM and N_2 adsorption analysis. The typical XRD pattern revealed a mesostructure of calcined TiO_2 shells with a strong peak at 2.5° 2θ, as shown in Figure 3(a). In addition, the formation of an anatase structure could be confirmed by XRD recorded at 20-40° (2θ). The TEM image at high magnification showed an array of mesopore channels over a large area (Fig. 3(b, c)). On the other hand, distorted pore channels were found in the stacked shell layers. The pore size distribution data calculated from the desorption branches of the nitrogen isotherms by the BJH method showed a mean pore diameter of approximately 3.7 nm. The shell of pure TiO_2 synthesized from Ti-MCM-41 sol showed BET surface areas of 462 m^2/g. The N_2 adsorption/desorption branch of mesoporous wall (Fig. 3(d)) exhibited a steep change in hysteresis with pressure, which is an indication of the presence of mesoporosity.

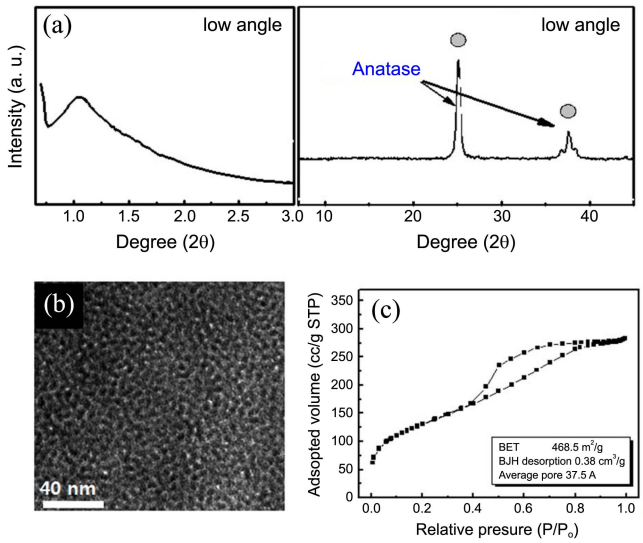

Figure 3. Typical XRD patterns (a), TEM image (b) and N_2 adsorption analysis result (c) for the hollow TiO_2.

The DNA adsorption was achieved effectively on the hollow type mesoporous pure TiO_2 microspheres as well as silica-TiO_2 mixed ones. Spectroscopic analysis was performed using the UV absorbance measurements for the resident solution (supernatant) to determine the binding amount of DNA on the TiO_2 surfaces after adsorption. The strong absorption bands at 260 nm derived from the basic component in DNA oligomers. The decrease in UV absorption band in solutions proved that DNA molecules had been bound progressively to the TiO_2 surfaces. As shown in Figure 4, the UV peak intensity at 260 nm decreased gradually and then disappeared with a prolonged time due to the removal of DNA in the solution through binding to the TiO_2 surfaces.

The effects of the TiO_2 contents and the porosity in the microcapsules on the adsorption rates and capacities of DNA were investigated, and the results are summarized in Figure 5. For this investigation, three types of hollow TiO_2 microcapsules with different amounts of silica and TiO_2 were fabricated. The DNA adsorption ability of the hollow type microcapsules containing TiO_2 components was dependent on the TiO_2 contents and the porosity of the samples. As the silica contents in the sample increased, the absorption

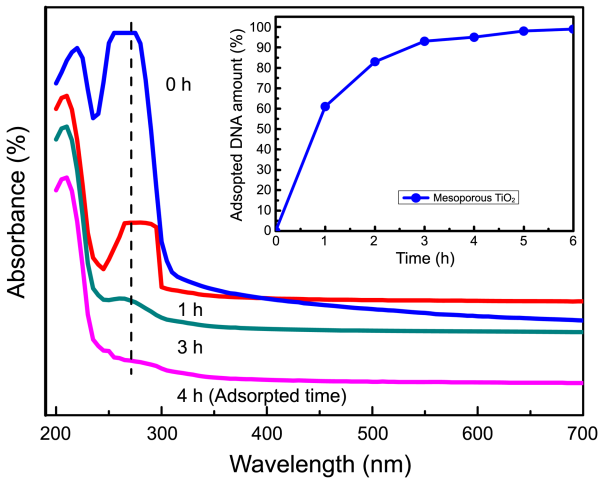

Figure 4. The change of peak intensity in UV spectra and the adsorpted amount of DNA on the TiO_2 surfaces with time.

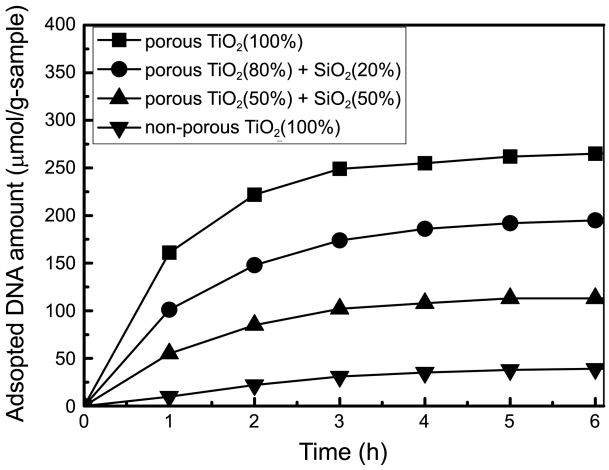

Figure 5. The effects of the TiO_2 contents and the presence of porosity on the adsorption rates and capacities of DNA over the hollow TiO_2 microcapsules.

ability decreased gradually. The adsorbed amount of DNA increased with increasing total contents of TiO_2 in the microcapsules. This shows that a higher TiO_2 contents in the hollow shells provided higher DNA adsorption sites. In addition, the mesoporous TiO_2 capsules showed 6-8 fold higher adsorption capability compared to the non-porous TiO_2 microspheres. The typically adsorbed maximum amount of DNA oligomer was 267.5 μmol/g-TiO_2 for the hollow type mesoporous Ti-MCM-41 capsules and 38.6 μmol/g-TiO_2 for the nonporous TiO_2 microspheres, respectively. This means that the porous anatase surfaces can provide large numbers of efficient sites for DNA adsorption compared to non-porous TiO_2. Nucleotides bind firmly to TiO_2 by complexation of their phosphate groups to the exposed titanium ions.[6] On the

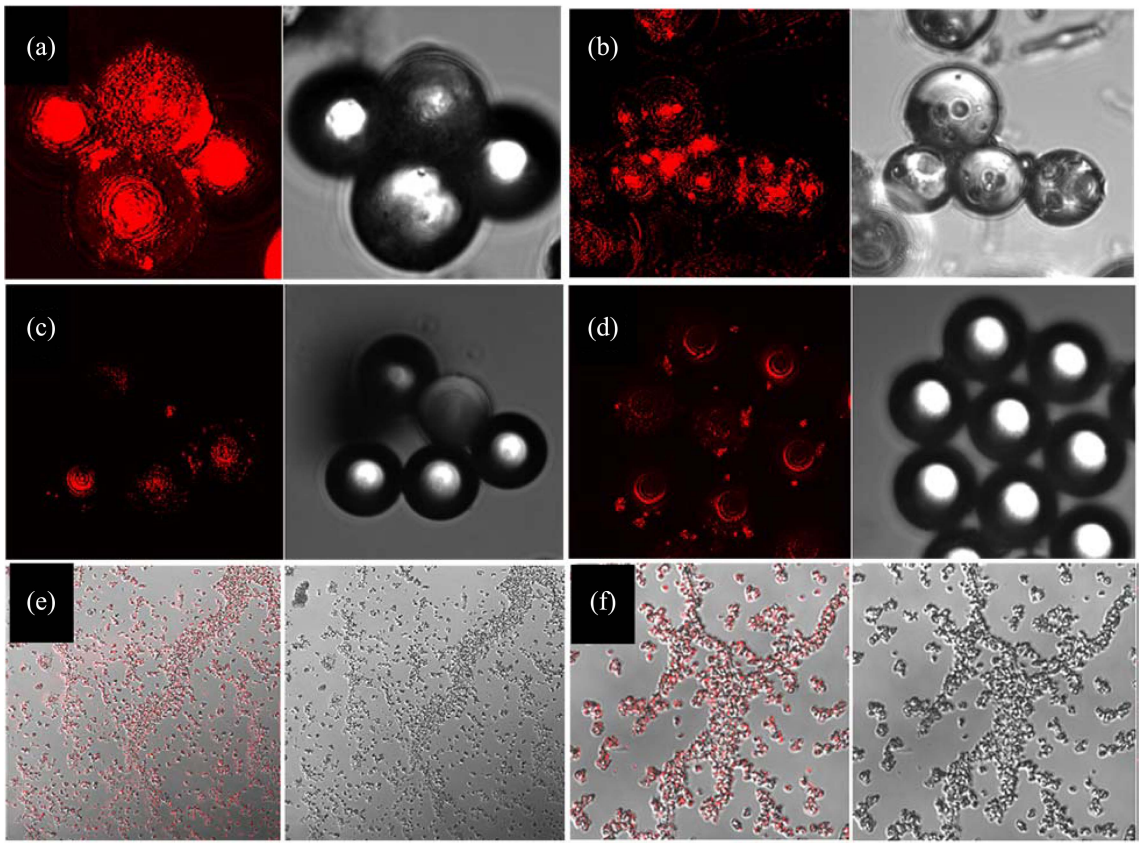

Figure 6. CLSM images for the cyanine(Cy5)-labeled DNA adsorpted on the TiO_2 surfaces. The distribution of red spots generated from the excited DNA. (a) mesoporous TiO_2 (b) mesoporous TiO_2(80%)+SiO_2(20%) (c) mesoporous TiO_2(50%)+SiO_2(50%) (d) non-porous TiO_2 (e) mesoporous pure TiO_2 (1.5 μm) (f) mesoporous pure TiO_2 (2.5 μm).

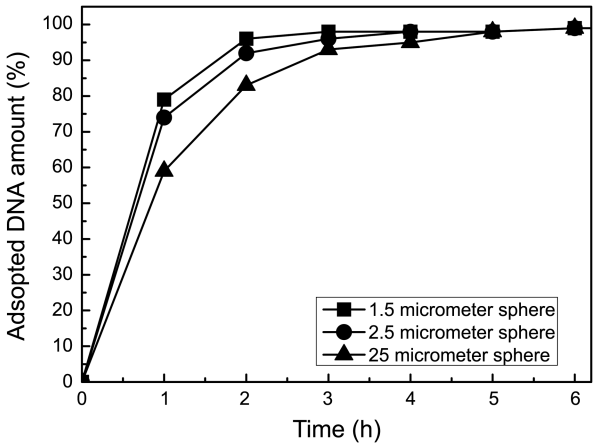

Figure 7. The effect of TiO_2 microcapsule size on the adsorption rates of DNA molecules.

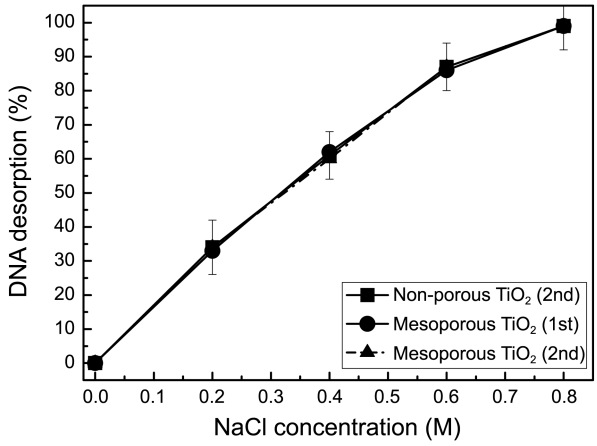

Figure 8. DNA desorption property from the TiO_2 surfaces using NaCl electrolyte as a function of concentration in solutions.

other hand, these mesoporous materials may offer the additional advantages, such as the size selectivity with respect to the target DNA by controlling the mesopore size.

The electrostatic interactions between the TiO_2 surfaces and target DNA labeled by cyanine (Cy5) were examined by confocal laser scanning microscopy (CLSM). The CLSM images can provide DNA adsorption efficiencies directly. Figure 6 shows the distribution of red spots generated from the excited DNA as a function of TiO_2 contents in the egg shell. The hollow spheres were composed of a mixture of silica and TiO_2, and those samples contained the nonporous TiO_2 particles. The right images in the photographs of Figure 6 were measured without emission in the same ranges. With increasing level of DNA adsorption, a high population of exiting red spots was observed in the CLSM images due to the increasing concentration of Cy5-labeled DNA bound to the TiO_2 surfaces. In Figure 6(a) and (b), the CLSM images confirmed that a higher exposure of TiO_2 surfaces is needed for the effective adsorption of DNA molecules. For the mesoporous Ti-MCM-41 (in Fig. 6(a) and (c)), the red color from the adsorbed DNA covers the entire surface area in the CLSM images, indicating the superior adsorption ability of mesoporous TiO_2 microcapsules to the nonporous ones. When silica was co-incorporated with TiO_2 for the mesoporous samples, the red color became deeper as the TiO_2 content was increased, as shown in Figure 6(c) and (d), indicating that the amounts of DNA adsorbed increased with increasing TiO_2 content in the microcapsules.

The effect of size in the TiO_2 microcapsules on the adsorption rates was investigated, and the results are compared in Figure 7. For this purpose, three types of hollow TiO_2 microcapsules with diameters of 1.5, 2.5 and 25 μm were tested. A higher DNA adsorption rate was obtained as the size of TiO_2 sample decreased. In addition, the mesoporous TiO_2 capsules, 1.5 μm in diameter, exhibited 1.5 times higher total adsorption capability compared to the 25 μm TiO_2 microspheres. This means that the larger porous surfaces can be provided because the diameter of TiO_2 microcapsules became smaller at the same weight of the samples.

DNA separation from the TiO_2 surfaces was investigated as a function of the NaCl concentration in the solution to alter the ionic strength for dissociation. The NaCl salt interacted with the phosphate backbones of DNA to decrease the bond strength between DNA and TiO_2 surface. Figure 8 shows the result for the DNA desorption property. The amount of DNA desorbed from the mesoporous TiO_2 particles increased with increasing concentration of the salt solution. The same trend was found for the nonporous TiO_2 microcapsules, as shown in Figure 8.

The TiO_2 microcapsules with the hollow macroporous core and mesoporous shell structure showed efficient ability to immobilize the DNA oligonucleotides. In particular, the mesoporous morphology of the anatase layers has many adsorption sites to increase the amount of immobilized probes on the surface. In addition, this material could be used as an active photo-catalyst for the decomposition of VOCs. Further studies to enlarge the application areas are currently underway.

Conclusion

In this study, pure TiO_2 microcapsules with a hollow core and a mesoporous shell were synthesized using PMMA polymer spheres after modifying their surfaces by non-thermal plasma. These microcapsules have a bimodal pore system of uniform and tunable hollow macroscopic cores with mesopores in the shells, and could be used as an efficient support to adsorb the Cy5-labeled DNA molecules. This material has a wide range of applications, including adsorbents, packing materials and photo-catalyst in the controlled system.

Acknowledgments. This research was supported in part by Research grant from the National Research Foundation of Korea (NRF), funded by the Korean Government (MEST) (No. 3148213322) and by a New & Renewable Energy of the Korea Institute of Energy Technology Evaluation and Planning (KETEP) grant funded by the Korea government

Ministry of Knowledge Economy (No. 20113030040010).

References

1. Kuhara, M.; Takeyama, H.; Tanaka, T.; Matsunaga, T. *Anal. Chem.* **2004**, *76*, 6207.
2. Park, S. J.; Taton, T. A.; Mirkin, C. H. *Science* **2002**, *295*, 1503.
3. Warner, M. G.; Hutchison, J. E. *Nat. Mater.* **2003**, *2*, 272.
4. (a) Steel, A. B.; Herne, T. M.; Tarlov, M. J. *Anal. Chem.* **1998**, *70*, 4670. (b) Boon, E. M.; Ceres, D. M.; Drummond, T. G.; Hill, M. G.; Barton, J. K. *Nat. Biotechnol.* **2000**, *18*, 1096. (c) Patolsky, F.; Lichtenstein, A.; Willner, I. *J. Amer. Chem. Soc.* **2001**, *123*, 5194. (d) Palecek, E.; Fojta, M. *Anal. Chem.* **2001**, 75A.
5. Kang, K.; Choi, J.; Nam, J. H.; Lee, S. C.; Kim, K. J.; Lee, S.-W.; Chang, J. H. *J. Phys, Chem. B* **2009**, *113*, 536.
6. Meier, K.-R.; Gratzel, M. *CHEMPHYCHEM* **2002**, *4*, 371.
7. Shinohara, H.; Gratzel, M.; Vlachopoulos, N.; Aizawa, M. *Bioelectrochem. Bioenerg.* **1991**, *26*, 307.
8. Bourgeat-Lami, E; Duguet, E. In *Functional Coatings by polymer microencapsulation*; Ghosh, S. K., Ed.; Wiley-VCH Verlag GmbH: Weinheim 2006; Vol. 4, p 85.
9. Jiang, P.; Berton, J. F.; Colvin, V. L. *Science* **2001**, *291*, 453.
10. Kim, S. W.; Kim, M.; Lee, W. Y.; Hyeon, T. *J. Am. Chem. Soc.* **2002**, *124*, 7642.
11. Velev, O. D.; Jede, T. A.; Lobo, R. F.; Lenhoff, A. M. *Nature* **1997**, *389*, 448.
12. Holland, B. T.; Blanford, C. F.; Stein, A. *Science* **1998**, *281*, 538.
13. Imhof, A.; Pine, J. *Nature* **1997**, *389*, 948.
14. Breulmann, M.; Davis, S. A.; Mann, S.; Hentze, H. P.; Antonietti, M. *Adv. Mater.* **2000**, *12*, 502.
15. Antonelli, D. M. *Microporous and Mesoporous Mater.* **1999**, *33*, 209.
16. Sepulveda, P.; Binner, G. P. J. *Eur. Ceram. Soc.* **1999**, *19*, 2059.
17. Davis, S. A.; Burkett, S. L.; Mendelson, N. H.; Mann, S. *Nature* **1997**, *385*, 420.
18. Lu, Y.; Fan, H.; Stump, A.; Ward, T.; Rieker, T.; Rinker, C. J. *Nature* **1999**, *398*, 223.
19. Gittins, D. I.; Caruso, F. *Adv. Mater.* **2001**, *13*, 740.
20. Wang, X. D.; Yang, W. I.; Tang, Y.; Wang, Y. J.; Fu, S. K.; Gao, Z. *Chem. Commun*. **2000**, 2161.
21. Deng, Z.; Chen, M.; Zhou, S.; Wu, L. *Langmuir* **2006**, *22*, 6403.
22. Yoon, H.; Hong, J.; Park, C. W.; Park, D. W.; Shim, S. E. *Mater. Lett.* **2009**, *63*, 2047.
23. (a) Kim, G. J.; Guo, X.-F. J. *Phy. Chem. Sol.* **2010**, *71*, 612. (b) Guo, X.-F.; Kim, Y.-S.; Kim, G. J. *J. Phys. Chem. C* **2009**, *113*, 8313.
24. Mu, J.; Zhou, Yu.; Bu, X.; Zhang, T. *J. Inorg. Organomet. Polym.* **2014**, *24*, 776.